Sensors & Transducers, Vol. 171, Issue 5, May 2014, pp. 232-238

www.sensorsportal.com

Sensors & Transducers

http://www.sensorsportal.com

Design of Meander Antenna for UHF Partial Discharge Detection of Transformers

[1] Mengjie Li, [1] Chuangxin Guo, [2] Ziping Peng

[1] College of Electrical Engineering, Zhejiang University, Hangzhou, Zhejiang Province 310027, China
[2] Zhongshan Power Supply Bureau, Guangdong Power Grid Corporation, Zhongshan 528400, China
[1] Tel.: +86-23-65111172, fax: +86-23-65102442
[1] E-mail: liuxhcd@126.com

Received: 6 May 2014 /Accepted: 27 May 2014 /Published: 31 May 2014

Abstract: Ultra high frequency (UHF) partial discharge (PD) detection approaches take advantages of strong anti-interference ability, and have been considered as a promising technology for online monitoring PD signals. This paper presents a meander antenna with wide frequency band and small size for UHF PD detection in power transformers. The optimal geometric parameters of the meander antenna were obtained through the parametric investigation. A prototype of the proposed antenna was fabricated. Actual PD experiments were carried out for typical artificial insulation defect models while the antenna was used for PD measurements. The experimental results show that the proposed meander antenna is suitable and effective for UHF online monitoring of PDs in transformers. *Copyright © 2014 IFSA Publishing, S. L.*

Keywords: Partial discharge, Transformer, Meander antenna, Parametric investigation, Ultra-high-frequency detection.

1. Introduction

Power transformers play very important roles in power systems. The faults of oil-paper insulation were the main cause of power transformers failures, which often start with partial discharges (PDs). By receiving the electromagnetic emissions of PD generate in a power transformer, the ultra-high frequency (UHF) detection technology can inspect insulation defects and identify potential faults in power transformer [1-5]. Compared with traditional detection methods, UHF technology has the advantage of strong anti-interference, which makes it immune to the radio frequency interferences (RFIs) from power line communication and corona discharges on high voltage terminals near transformers [6, 7]. UHF antenna is core component in the PD online detection systems because the performance of antenna will affect the extraction and post-processing of PD signals.

Different from the antennas in communication applications, the impedance bandwidth of UHF PD antennas are required to fall into the range between 300 MHz and 1 GHz. For this reason, the UHF antennas in PD detection usually have a much larger size. At present, the UHF antennas used in PD detection can be divided into two kinds according to the installation location, which are external antennas and internal antennas. The external antennas include two-wire Archimedean planar spiral antenna [8], circular plate antennas [9] and a circular ring [10], etc. Those antennas can meet the demand for PD detection in transformers, but their diameters are too large, usually more than 20 cm, to be installed in transformers. The internal antennas have advantages such as strong anti-interference and high

sensitivity. But it requests the internal antennas have small size and good performance. The internal antennas were reported widely include Hilbert fractal antenna [11], Peano fractal antenna [12], disc sensor [13] and probe antenna [14], etc. However, those antennas have some shortages, such as narrow bandwidth and low gain etc. For an example, the impedance bandwidth of Hilbert fractal antenna [7] with side length of 100 mm is only a few hundred MHz between 300 MHz and 1 GHz, which would cause some loss of PDs information during PD detection. This motivates us to investigate an optimal antenna for UHF online monitoring of PDs with wider impedance bandwidth between 300 MHz and 1 GHz and even smaller dimensions.

The meander-line method was confirmed effective way for size reduction and wideband performance of the antenna. In recent years, as a simplified form of fractal antenna, meander-line antenna has been very hot in antenna design field. This paper presents a meander antenna for online monitoring of PDs in transformers which stems from the meander line wearable antenna [15] used in mobile communication systems. This new antenna has simple structure, small size and comparatively wide frequency bandwidth. The structure parameters of the meander antenna were carried out by simulation. A prototype of the proposed antenna was fabricated, and the application of the antenna for PD detection was validated through actual PD experiments with typical artificial insulation defect models in laboratory.

The paper is organized as follows: Section 2 presents the configuration of the proposed UHF PD antenna for power transformers. The parametric of the antenna was investigated in Section 3. Section 4 presents the prototype of the proposed antenna and its performance. Section 5 presents the PD experiments and results. The conclusion is given in Section 6.

2. Antenna Configuration

Meander-line antenna could obtain high radiation frequency through small size. The geometry of the proposed meander antenna is shown in Fig. 1.

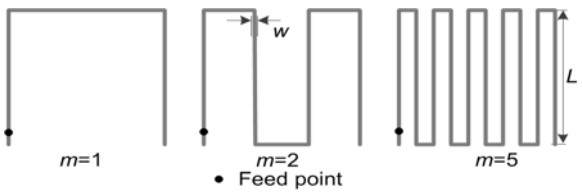

Fig. 1. Meander antenna curves of different order.

The antenna with a square shape of $L \times L$ mm^2, it is clear that the length of a meander curve is larger if the order of the curve is higher. The antenna was printed on a FR4 substrate with relative permittivity 4.4 and loss tangent 0.02. Compared with other antennas such as fractal antenna, the antenna has small size, simple structure and low cost. Moreover, it could be used for PD detection in transformers after optimization.

3. Parametric Investigation

To well understand the performance of a meander antenna, the effects of vital structural parameters such as the side dimension *L*, order of antenna *m*, width of conductor *w*, thickness *b* of the printed circuit board (FR4) on which the antenna lies and feed-point are thoroughly investigated by employing the commercially available software Ansoft® Designer. By conducting these parametric investigations, the antenna with desired performance can be anticipated for future after necessary modification.

The antenna simulation model in Ansoft® is shown in Fig. 2. The antenna contains 3 layers, which includes copper conductor, substrate (FR4 epoxy board with dielectric constant of 4.4), ground plane and probe feed.

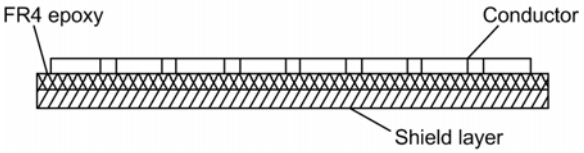

Fig. 2. Simulation model of the meander antenna.

3.1. Effects of the Antenna Side Dimension *L*

First, four different side dimensions (*L*=60 mm, 70 mm, 80 mm, 90 mm) of meander antenna were selected for study. For each side dimension L, structural parameters such as *w*=1.25 mm, *b*=0.7 mm and *m*=15 being identical. The simulated VSWR curve and gain curve of the proposed antenna when tuning the width of conductor were presented in Fig. 3. Side dimensional has great impact on antenna standing wave ratio as shown in Fig. 3 (a). As the decrease of side dimension, the antenna standing wave ratio was shift linearly to a higher frequency. The less the side dimensional of antenna was, and the higher the antenna standing wave ratio is. When the side dimensional of antenna is less than 70 mm, the standing wave ratio spike in the high frequency portion can be avoid avoided and the ideal VSWR curve can be obtained. The gain of the antenna was shown in Fig. 3 (b). As the decrease of side dimension, the antenna gain was also shift linearly to a higher frequency. The less the side dimensional of antenna is, and the lower the antenna standing wave ratio is.

3.2. Effects of the Antenna Order *m*

The order of antenna *m* decides the total length of conductor line. Other shown parameters unchanged, changing the order of antenna m, the relationship of VSWR and gain curves were shown in Fig. 4. From the graph, it is obvious that the order of antenna has significant impact to the VSWR curve. As the increase of antenna order, the antenna standing wave ratio decrease quickly, especially for low frequency. However, the gain of the antenna is not influenced by the order of antenna.

3.3. Effects of the Conductor Width *w*

The simulated VSWR curve and gain curve of the proposed antenna when tuning the width of conductor were presented in Fig. 5. In these figures, structural parameters such as *L*=70 mm, *b*=0.7 mm and *m*=15 being identical, except the conductor widths changed from 1 mm to 1.5 mm with a step increment of 0.25 mm. It has been shown in this study that the VSWR curve is most flat when the width of the conductor is 1.25 mm and changes greatly either higher than 1.5 mm or lower than 1.25 mm. A step increment of 0.25 mm for parameter *w* will allow the VSWR curves shifting linearly to a higher frequency, and will make the gain of the antenna increase to some extent, which are illustrated in Fig. 5 (b).

3.4. Effects of the Substrate Thickness *b*

When other parameter kept unchanged, namely *L*=70 mm, *m*=15, *w*=1.25 mm, tuning the thickness of substrate *b*, the change of VSWR and gain curves were shown in Fig. 6. In Fig. 6 (a), a 0.2 mm step increment in *b* from 0.5 to 1.1 mm will result in the VSWR curves was changed from oscillating to flat and to oscillating again, with turning point of *b*=0.7 mm. At the same time, as the increase of thickness, the standing-wave ratio increase gradually. As shown in Fig. 6 (b), for substrate in different thickness, the gain of antenna changes similarly that is the gain tends to increase as the thickness increase.

4. Optimization of a Meander Antenna

Based on the aforementioned parametric studies, the following design guidelines can be concluded.

1) The simulated VSWR curve and gain curve of the proposed antenna can be varied obviously by tuning parameters *L* and the order of antenna *m*.

2) Tuning parameters *w* and *b* can change the VSWR curve oscillation and change the standing-wave ratio and gain to some extent. Relevant steady standing-wave ratio could be obtained by regulating *w* and *b*.

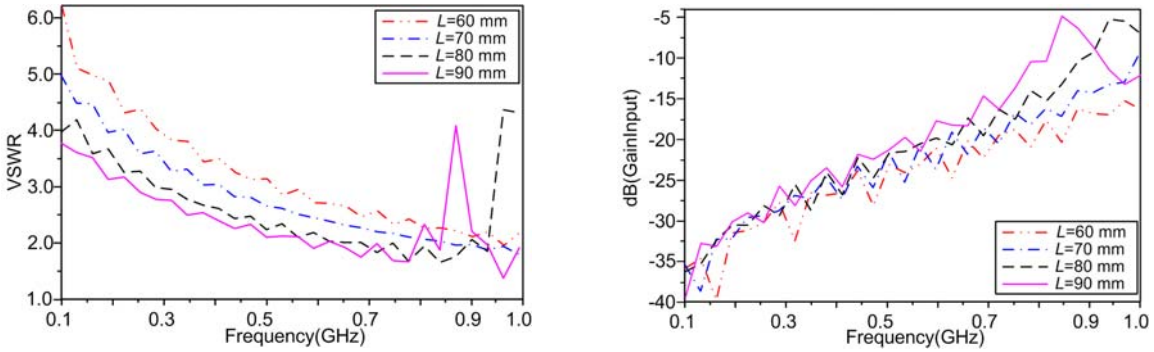

Fig. 3. The simulated VSWR curve and gain curve of antenna with different side dimension. (a) VSWR curves, (b) Gain curves.

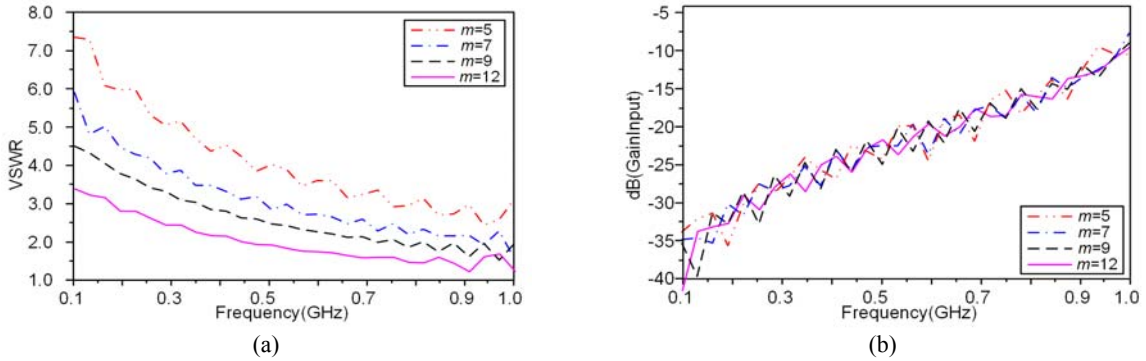

Fig. 4. The simulated VSWR curve and gain curve of antenna with different order. (a) VSWR curves, (b) Gain curves.

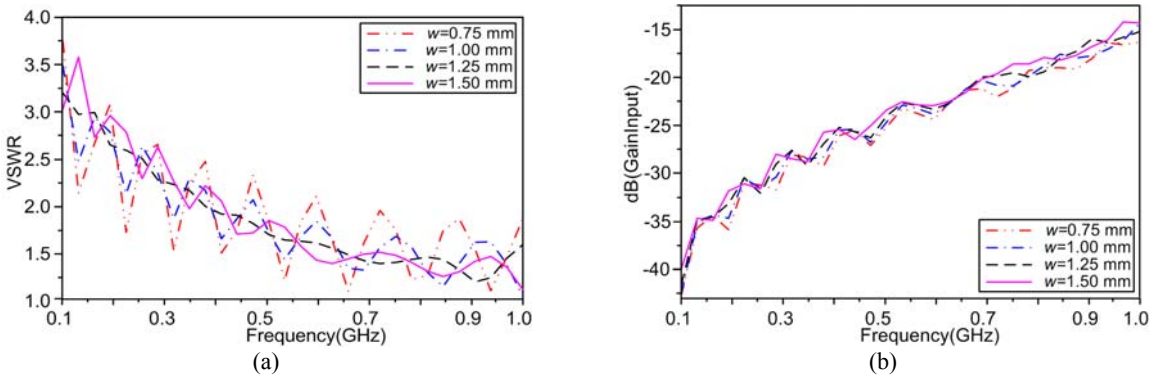

Fig. 5. The simulated VSWR curve and gain curve of antenna with different conductor width. (a) VSWR curves, (b) Gain curves.

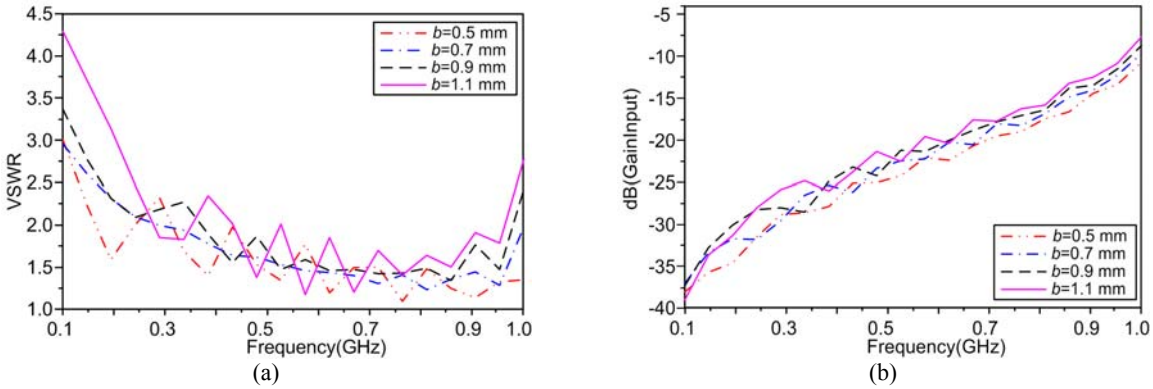

Fig. 6. The simulated VSWR curve and gain curve of antenna with different substrate thickness. (a) VSWR curves, (b) Gain curves.

3) Furthermore, the simulation result shows that the influence of distributing feed point to the performance of antenna has no regularity. The feed point 1, as shown in Fig. 7, was chosen in a number of simulation results.

Through the simulations, the parameters of the optimal antenna are determined as L=70 mm, w=1.25 mm, b=0.7 mm and the order of antenna m=15. The prototype of the proposed antenna was fabricated as shown in Fig. 7, and the size is 70 mm×70 mm×0.7 mm. Fig. 8 shows the voltage standing wave ratio (VSWR) of the proposed antenna.

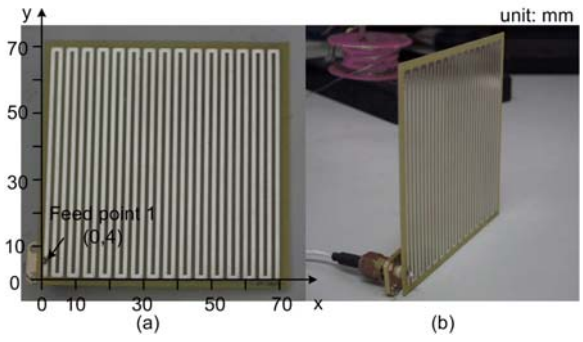

Fig. 7. The prototype of the proposed antenna: (a) front view of antenna, (b) side view of antenna.

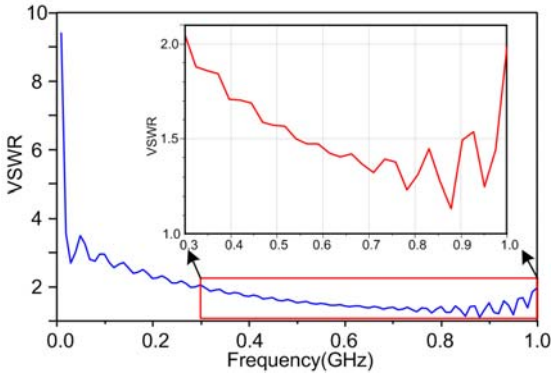

Fig. 8. The VSWR curve of the optimal antenna.

In 300 MHz~1 GHz, the VSWR is less than 2. The antenna has a pass frequency bandwidth of 700 MHz from 300 MHz to 1 GHz, which reached the requirement of wideband antenna. The simulation regain of the proposed antenna was also proved to be good. In 400 MHz~1 GHz, the gain is more than -25 dB and above 700 MHz, more than -20 dB. The three-dimensional and two-dimensional radiation patterns (phi=0 and 90 deg) at the frequencies of 400 MHz and 700 MHz, as shown in Fig. 9 and Fig. 10, respectively. The directivity of the antenna at the three frequencies is all nearly hemisphere and

the gain variations at the three frequencies are relatively stable. Therefore the antenna could receive electromagnetic wave from all directions, which benefit to PD detection. The simulation results also show that the antenna can match with a 50 Ω coaxial cable well in the pass bands.

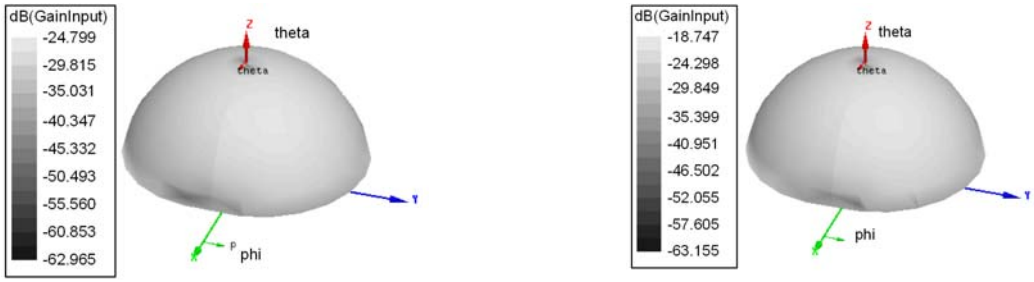

Fig. 9. The 3-D radiation pattern of the optimal antenna.

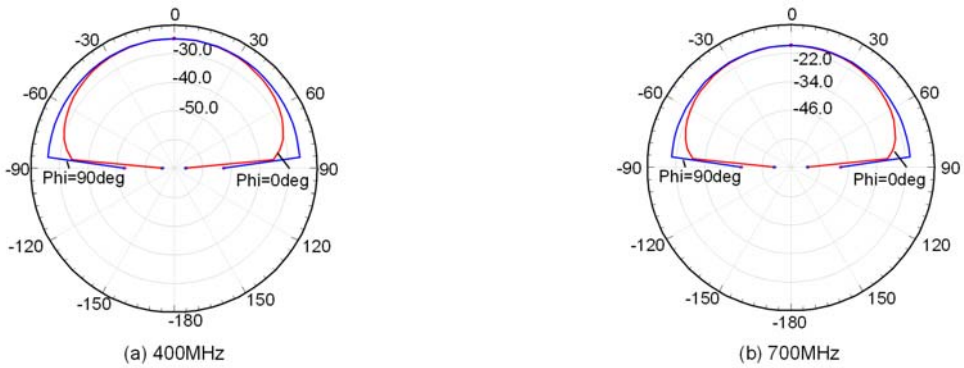

Fig. 10. The 2-D radiation pattern of the optimal antenna.

5. Partial Discharge Experiments and Results

To assure that the proposed antenna can be successfully applied to PD detection. The designed meander UHF antenna was used in laboratory for measuring PD caused by two artificial insulation defect models, namely air cavity discharge and surface discharge defects in oil. The experiment setup of UHF PD detection is shown in Fig. 11.

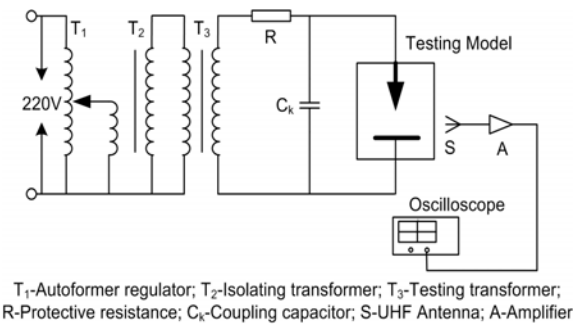

Fig. 11. The PD experiment setup in laboratory.

The artificial defect models were placed into an organic glass container filled with transformer oil. The UHF antenna was located in the vicinity of the testing models, with a distance of 50 mm between them. A digital oscilloscope with sampling frequency of 5 GHz was utilized to record the PD signals. The trigger time of the oscilloscope was set to 100 ns. All experiments were carried out in an electromagnetic shielded laboratory.

During the experiment, the PD signals were collected when discharge sufficiently. Fig. 12 (a-1) and Fig. 12 (b-1) show the examples of UHF PD signals of the defect models detected by meander UHF antenna. The UHF PD signals of the two defected models are look similar in frequency spectra but different in details. Normalized power spectra of the UHF PD signals are shown in Fig. 12 (a-2) and Fig. 12 (b-2). The results show that the power spectra among different defect models are obviously different, which can be used for partial discharge pattern recognition by analysis to the waveforms. Besides, the pass frequency bands of the proposed antenna are between 300 MHz and 1 GHz, which means the UHF PD signals detected by the proposed antenna contain more information than those multiband antennas. The partial discharge experiments indicate that the proposed antenna is effective in capturing PD waveforms.

During the experiment, the PD signals were collected when discharge sufficiently. Fig. 12 (a-1)

and Fig. 12 (b-1) show the examples of UHF PD signals of the defect models detected by meander UHF antenna. The UHF PD signals of the two defected models are look similar in frequency spectra but different in details. Normalized power spectra of the UHF PD signals are shown in Fig. 12 (a-2) and Fig. 12 (b-2). The results show that the power spectra among different defect models are obviously different, which can be used for partial discharge pattern recognition by analysis to the waveforms. Besides, the pass frequency bands of the proposed antenna are between 300 MHz and 1 GHz, which means the UHF PD signals detected by the proposed antenna contain more information than those multiband antennas. The partial discharge experiments indicate that the proposed antenna is effective in capturing PD waveforms.

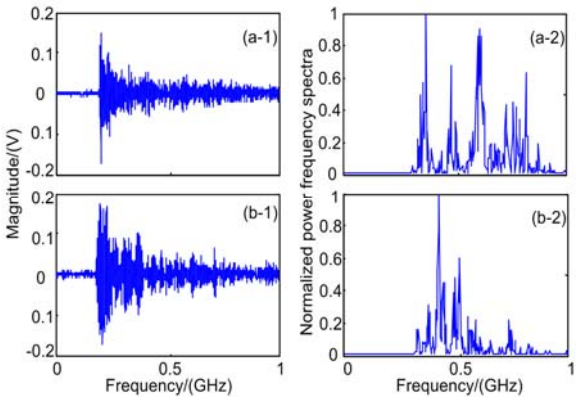

Fig. 12. Waveforms and normalized power frequency spectra of UHF PD signals: (a) Surface discharge-in-oil mode1, (b) Gas-cavity discharge model.

6. Conclusions

According to the demand of PD detection in power transformers, this paper presents a meander UHF antenna. A detailed parametric investigation of the VSWR bandwidth and gain of the proposed antenna has been implemented. The actual antenna was fabricated based on the optimal design procedure. The actual PD experiments involving two typical artificial insulation defect models were carried out to verify the performance of the antenna. The results of the work can be summarized as follows:

a) The pass frequency bands of the meander antenna are approximate 300 MHz~1 GHz, which reached the requirement of wideband antenna. The meander antenna can effectively detect the PD signals and attenuate the signals below 300 MHz.

b) The radiation patterns show that the meander antenna can receive electromagnetic waves from the front of the antenna. The gain variations of the optimal antenna at the three frequencies are relatively stable.

c) The experimental results show that the proposed antenna is effectively applied for UHF PD online monitoring of transformers. And the UHF PD signals measured by the proposed antenna can be used for recognition of PDs.

Acknowledgements

This work was supported in part by State Key Development Program for Basic Research of China (2013CB228206). National Natural Science Foundation of China (51177143) and Zhejiang Province Natural Science Key Foundation (LZ12E07002) are also appreciated for supporting this work.

References

[1]. D. Aschenbrenner, H. G. Kranz, W. R. Rutgers, P. Van Den Aardweg, On line PD measurements and diagnosis on power transformers, *IEEE Transactions on Dielectrics and Electrical Insulation*, 12, 2005, pp. 216-222.

[2]. T. Pinpart, M. D. Judd, Differentiating between partial discharge sources using envelope comparison of ultra-high-frequency signals, *IET Science, Measurement and Technology*, 4, 2010, pp. 256-267.

[3]. R. Sarathi, G. Koperundevi, UHF technique for identification of partial discharge in a composite insulation under AC and DC voltages, *IEEE Transactions on Dielectrics and Electrical Insulation*, 15, 2008, pp. 1724-1730.

[4]. Y. Shibuya, S. Matsumoto, M. Tanaka, H. Muto, Y. Kaneda, Electromagnetic waves from partial discharges and their detection using patch antenna, *IEEE Transactions on Dielectrics and Electrical Insulation*, 17, 2010, pp. 862-871.

[5]. S. Tenbohlen, D. Denissov, S. M. Hoek, S. M. Markalous, Partial Discharge Measurement in the Ultra High Frequency (UHF) Range, *IEEE Transactions on Dielectrics and Electrical Insulation*, 15, Dec. 2008, pp. 1544-1552.

[6]. W. Gao, D. Ding, W. Liu, Research on the typical partial discharge using the uhf detection method for GIS, *IEEE Transactions on Power Delivery*, 26, 2011, pp. 2621-2629.

[7]. J. Li, T. Jiang, C. Wang, C. Cheng, Optimization of UHF Hilbert antenna for partial discharge detection of transformers, *IEEE Transactions on Antennas and Propagation*, 60, 2012, pp. 2536-2540.

[8]. W. Wei, T. Zhiguo, C. Li, X. Huang, X. Li, Research on PD Detection in Power Transformers Using UHF, *High Voltage Engineering*, 29, 2003, pp. 32-34.

[9]. C. Sun, G. Xu, J. Tang, H. Shi, W. Zhu, Model and Performance of Inner Sensors Used for Partial Discharge Detection in GIS, in *Proceedings of the CSEE*, 24, 2004, pp. 92-97.

[10]. J. Tang, H. Shi, C. Sun, G. Wei, W. Zhu, Study of UHF frequency response characteristics of the inner sensor for partial discharge detection in GIS, *Diangong Jishu Xuebao/Transactions of China Electrotechnical Society*, 19, 2004, pp. 71-75.

[11]. J. Li, T. Jiang, C. Cheng, C. Wang, Hilbert Fractal Antenna for UHF Detection of Partial Discharges in Transformers, *IEEE Transactions on Dielectrics and Electrical Insulation*, 20, Dec. 2013, pp. 2017-2025.

[12]. J. Li, C. Cheng, L. Bao, T. Jiang, Resonant frequency calculation and optimal design of peano fractal antenna for partial discharge detection, *International Journal of Antennas and Propagation*, Vol. 2012, 2012, 361517.
[13]. L. Gu, J. Chen, W. Liu, J. Lu, M. Chen, Y. M. Li, Impact Factors of Disc Sensor for Partial Discharge in GIS, *High Voltage Apparatus*, 48, 2012, pp. 55-59.
[14]. F. Marangoni, J. P. Reynders, P. J. De Klerk, Investigation into the effects of different antenna dimensions for UHF detection of partial discharges in power transformers, in *Proceedings of the IEEE Power Tech Conference*, Bologna, Italy, 23-26 June 2003, pp. 1048-1053.
[15]. G. George, R. Nagarjun, D. Thiripurasundari, R. Poonkuzhali, Z. C. Alex, Design of meander line wearable antenna, in *Proceedings of the IEEE Conference on Information and Communication Technologies* (*ICT'13)*, Thuckalay, Tamil Nadu, India, 11-12 April 2013, pp. 1190-1193.